Organic Electronics 38 (2016) 370–378

Contents lists available at ScienceDirect

Organic Electronics

journal homepage: www.elsevier.com/locate/orgel

Friedel-Crafts arylmethylation: A simple approach to synthesize bipolar host materials for efficient electroluminescence

Chang-Jin Ou [a, b], Jin-Yi Lin [a, b], Jie Mao [b], Shuang-Quan Chu [b], Yu Zhao [b], Ling-Hai Xie [b, **], Hong-Tao Cao [b], Xin-Wen Zhang [b, ***], Ying Wei [b], Wei Huang [a, b, *]

[a] Key Laboratory of Flexible Electronics (KLOFE), Institute of Advanced Materials (IAM), Jiangsu National Synergetic Innovation Center for Advanced Materials (SICAM), Nanjing Tech University, Nanjing 211816, China

[b] Institute of Optoelectronic Materials (IOM), Key Laboratory for Organic Electronics & Information Displays (KLOEID), Institute of Advanced Materials (IAM), Jiangsu National Synergetic Innovation Center for Advanced Materials (SICAM), Nanjing University of Posts & Telecommunications, Nanjing 210046, China

A R T I C L E I N F O

Article history:
Received 20 June 2016
Received in revised form
15 August 2016
Accepted 18 August 2016

Keywords:
Bipolar host materials
Sulfone
Friedel-Crafts arylmethylation
Solution process

A B S T R A C T S

In order to simplify the synthesis of bipolar host materials of OLEDs, a facile synthetic approach was developed and a series of sulfone-contained bipolar host materials were synthesized via mild one-step Friedel-Crafts arylmethylation. Due to π-conjugate-interrupted connection between donor moiety and sulfone moiety, those materials keep high triplet energy and separate the HOMO and LUMO levels. Furthermore, the introduction of sulfone group can significantly lower LUMO level. Based on newly synthesized sulfone-based bipolar host materials, efficient solution-processed sky-blue phosphorescent OLEDs were fabricated with high current efficiency of 16.5 cd/A. Our results demonstrate Friedel-Crafts arylmethylation is powerful synthetic strategy to construct bipolar host materials.

1. Introduction

The study enthusiasm on phosphorescence and thermally-activated delayed fluorescence (TADF)-based OLEDs is soaring since both can simultaneously harvest singlet and triplet excitons, which enables a 100% internal quantum efficiency [1–3]. While, due to long lifetime of triplet excitons, triplet-triplet annihilation and triplet-polaron annihilation become serious problems at high exciton density in both PhOLEDs and TADF OLEDs [4]. In order to solve the problems, the emitters should be dispersed into a host material with higher triplet energy level at low doped concentration to confine triplet excitons on emitters. Numerous studies demonstrate that bipolar host materials, incorporating electron-donating (D) and electron-accepting (A) components into molecule structures, can facilitate and balance the injection and transport of carriers, which determines the quantum efficiency of devices [5–10].

Phosphine oxide (PO) group is widely used to construct bipolar host materials, which have exhibited excellent device performance, while PO-based materials are synthesized via multiple steps [11–15]. Novel synthetic approaches should be developed to simplify synthesis and meet the need of commercialization of OLEDs. Lee and Kim groups respectively reported 4,5-diazofluorenone and thioxanthe-9-one-S,S-dioxide condensed with carbazole derivatives under acid catalysis and afforded bipolar host materials [16,17]. Huang group reported highly efficient blue PhOLEDs with maximum current efficiency of 42.1 cd/A based on carbazole-pyridine hybridized bipolar host materials, which were synthesized via one-step C—N coupling approach [18]. Generally, D components of bipolar host material, such as carbazole, triphenylamine, dibenzothiophene, are typically synthetic precursors for Friedel-Crafts (FC) reaction [19–21]. In addition, the D and A synthons are available individually, and can be freely combined via rational molecular design to construct a desired bipolar host material. So one-step FC arylmethylation may be an intriguing reaction to construct efficient bipolar host materials. Quan et al. reported 4,5-diazofluorene-9-ol (A synthon) facile attached to

---

* Corresponding author. Key Laboratory of Flexible Electronics (KLOFE), Institute of Advanced Materials (IAM), Jiangsu National Synergetic Innovation Center for Advanced Materials (SICAM), Nanjing Tech University, Nanjing 211816, China.

** Corresponding author.

*** Corresponding author.

E-mail address: iamwhuang@njupt.edu.cn (W. Huang).

http://dx.doi.org/10.1016/j.orgel.2016.08.018
1566-1199/

triphenylamine (D synthon) via sulfuric acid-catalyzed FC arylmethylation, and they found the number of A component in host material affects device current efficiency dramatically [22]. Our group has utilized FC arylmethylation to construct several kinds of bipolar materials [23–25]. Huang et al. developed bulky 9-pyridinylfluorenyl moiety functionalized bipolar host materials via FC arylmethylation [24]. However, due to lack of A synthons of FC arylmethylation and harsh reaction condition, researchers have paid less attention to this synthetic strategy.

Nowadays, sulfone has become attractive building block in bipolar host materials and TADF emitters due to outstanding electron-accepting and transporting ability [17,26–34]. Kim [14], Poriel [28] and Su [29] groups respectively reported sp3-C connected thioxanthene 10,10-dioxide with carbazole or triphenylamine bipolar host materials, showing separated HOMO and LOMO energy levels, and high current efficiency of over 20 cd/A in Firpic-based sky-blue PhOLEDs. However, there is still a lacks of a general and convenient approach to construct sulfone-based bipolar host materials. Herein, two sulfone-contained A synthons, 9-hydroxy-9-phenylthioxanthene 10,10-dioxide and 9-hydroxy-9-(4-(octyloxy)phenyl)thioxanthene 10,10-dioxide, were synthesized via directed *ortho*-metalation of diphenyl sulfone. Those A synthons can effectively link to D synthons, and construct bipolar host materials under mild $BF_3\cdot Et_2O$-mediated FC arylmethylation. Finally, efficient solution-processed sky-blue PhOLEDs were fabricated with high current efficiency of 16.5 cd/A based on synthesized bipolar host materials.

2. Experimental section

2.1. Materials and instruments

All of chemicals were purchased from J&K Scientific Co. Ltd., and were used without further purification unless otherwise state. Anhydrous THF was distilled from Na/benzophenone.

1H NMR and 13C NMR spectra were measured on a Varian Mercury Plus 400 spectrometer with tetramethylsilane as the internal standard. Absorption and photoluminescence spectra were measured in dichloromethane solution using a SHIMADZU UV-3600 spectrophotometer and a SHIMADZU RF-5301PC spectrophotometer, respectively. Low-temperature phosphorescence were measured in 2-methylTHF at 77 K using a HITACHI F4600 spectrophotometer. Thermogravimetric analysis (TGA) was undertaken with a Shimadzu thermogravimetry and differential thermal analysis DTG-60H at a heating rate of 10 °C/min under N_2. Differential scanning calorimetry (DSC) measurements were performed under a nitrogen atmosphere at both heating and cooling rates of 10 °C/min, using Shimadzu DSC-60A. Elemental analyses were recorded at the Vario EL III (Elemeraor Co. Ltd, Germany). FT-IR spectra were recorded at Shimadzu IRPrestige-21. The single crystal data collection was performed at 100 or 298 K on a Bruker 2000 CCD area detector using graphite-monochromated Mo Kα radiation ($\lambda = 0.71073$ Å). All structures were solved by direct methods using SHELXS-2014 and refined against F^2 using SHELXL-2014. Hydrogen atoms were fixed geometrically and refined isotropically. CCDC No. of PhSOH, OPhSOH, 1c, 1d and 1e are 1,473,561, 1,473,563, 1,479,132, 1,473,566 and 1,479,421, respectively.

2.2. Synthesis

9-hydroxy-9-phenylthioxanthene 10,10-dioxide (PhSOH). Diphenyl sulfone (7.2 g, 33 mmol) was dissolved in anhydrous THF solution (200 mL) and stirred at dry ice-alcohol bath, and then 2.5 M *n*-BuLi/n-hexane solution (27.7 mL, 69.3 mmol) was added slowly. Methyl 4′-bromobiphenyl-2-carboxylate (4.08 g, 30 mmol) was added into reaction after 3 h. Removing cool bath and stirring at room temperature about 24 h, then saturated NH4Cl solution was added to quench and hydrolyze, and extracted with dichloromethane. The combined organic abstract was dried over anhydrous MgSO4 and filtered. The solution was evaporated under vacuum condition and the crude product was purified by silica gel column chromatography to afford white solid (9.4 g) with 88.0% yield. 1H NMR (400 MHz, $CDCl_3$) δ 8.11 (d, $J = 7.6$ Hz, 2H), 7.94 (d, $J = 8.0$ Hz, 2H), 7.64 (dd, $J = 7.6$, 1.6 Hz, 2H), 7.56 (dd, $J = 7.6$, 1.2 Hz, 2H), 7.28–7.24 (m, 5H), 3.23 (s, 1H); 13C NMR (100 MHz, $CDCl_3$) δ 143.93, 143.63, 136.06, 132.92, 128.86, 128.44, 128.18, 127.89, 126.80, 123.69, 74.09. IR (KBr): $\upsilon = 3452$ (O–H), 3057 (Aryl C–H), 1593 (Aryl C=C), 1581 (Aryl C=C), 1494 (Aryl C=C), 1469 (Aryl C=C), 1448 (Aryl C=C), 1437 (Aryl C=C), 1377 (O–H), 1280 ($-SO_2-$), 1213, 1157 ($-SO_2-$), 1142 (C–O), 1026, 906, 870, 760, 746, 594 cm^{-1}.

9-hydroxy-9-(4-(octyloxy)phenyl)thioxanthene 10,10-dioxide (OPhSOH). The synthetic procedure is similar to PhSOH, and afford light yellow solid product (8.5 g) with 72.1% yield. 1H NMR (400 MHz, $CDCl_3$) δ 8.11 (dd, $J = 7.6$, 1.2 Hz, 2H), 8.00 (d, $J = 8.0$ Hz, 2H), 7.65 (td, $J = 7.6$, 1.2 Hz, 2H), 7.56 (t, $J = 7.6$ Hz, 2H), 7.10 (d, $J = 9.2$ Hz, 2H), 6.74 (d, $J = 9.2$ Hz, 2H), 3.86 (t, $J = 6.8$ Hz, 2H), 3.17 (s, 1H), 1.75–1.68 (m, 2H), 1.42–1.35 (m, 2H), 1.30–1.24 (m, 8H), 0.87 (t, $J = 6.8$ Hz, 3H). 13C NMR (100 MHz, $CDCl_3$) δ 158.85, 144.03, 135.99, 135.92, 132.83, 128.69, 128.19, 127.54, 123.75, 114.19, 73.95, 67.96, 31.79, 29.30, 29.20, 29.17, 26.00, 22.63, 14.08. IR (KBr): $\upsilon = 3506$ (OH), 3066 (Aryl CH), 2922 (CH_2, CH_3), 2854 (CH_2, CH_3), 1608 (Aryl C=C), 1579 (Aryl C=C), 1506 (Aryl C=C), 1465 (Aryl C=C), 1441 (Aryl C=C), 1392 (CH_3), 1288 ($-SO_2-$), 1248 (Ar-O-R), 1153 ($-SO_2-$), 1136 (C–O), 1043, 1024, 910, 825, 763, 756, 626, 592 cm^{-1}.

Synthesis of 1b. 9-phenylcarbazole (0.97 g, 4 mmol) and OPhSOH (0.45 g, 1 mmol) were dissolved in anhydrous dichloromethane solution (50 mL). Then, the $BF_3\cdot Et_2O$ (0.14 g, 1 mmol) was added slowly into the reaction mixture. Large amount of water was added to quench reaction after 8 h, and extracted with dichloromethane. The combined organic abstract was dried over anhydrous MgSO4 and filtered. The solution was evaporated under vacuum condition and the crude product was purified by silica gel column chromatography to afford light yellow solid (0.61 g) with 91.0% yield. 1H NMR (400 MHz, $CDCl_3$) δ 8.22 (dd, $J = 7.6$, 1.2 Hz, 2H), 7.89 (d, $J = 7.6$ Hz, 1H), 7.59–7.55 (m, 5H), 7.55–7.51 (m, 2H), 7.50–7.44 (m, 3H), 7.41–7.35 (m, 2H), 7.28 (d, $J = 8.8$ Hz, 2H), 7.24–7.19 (m, 1H), 7.13 (d, $J = 8.0$ Hz, 2H), 6.84 (dd, $J = 8.8$, 1.8 Hz, 1H), 6.81–6.74 (m, 4H), 3.93 (t, $J = 6.4$ Hz, 2H), 1.83–1.71 (m, 2H), 1.47–1.40 (m, 2H), 1.33–1.26 (m, 8H), 0.88 (t, $J = 6.8$ Hz, 3H). 13C NMR (100 MHz, $CDCl_3$) δ 158.08, 146.37, 141.29, 139.75, 137.51, 137.32, 136.88, 136.18, 132.01, 131.68, 131.23, 129.87, 128.60, 127.82, 127.54, 126.96, 126.16, 124.02, 123.19, 122.77, 122.39, 120.36, 120.04, 113.92, 109.93, 109.35, 67.97, 58.64, 31.82, 29.37, 29.31, 29.24, 26.09, 22.65, 14.10. MALDI-TOF MS: calculated for $C_{45}H_{41}NO_3S$ 675.88; found: 675.14 (M+). Elemental analysis calculated for $C_{45}H_{41}NO_3S$: C, 79.97%; H, 6.11%; N, 2.07%; O, 7.10%; S, 4.74%. Found: C, 80.10%; H, 6.19%; N, 2.25%. IR (KBr): $\upsilon = 3061$ (aryl CH), 2926 (CH_2, CH_3), 2854 (CH_2, CH_3), 1597 (Aryl C=C), 1502 (Aryl C=C), 1456 (Aryl C=C), 1440 (Aryl C=C), 1361, 1307 ($-SO_2-$), 1249 (Ar-O-R), 1234 (Ar-N-Ar), 1165 ($-SO_2-$), 1145, 1056, 827, 758, 731, 698, 584, 572 cm^{-1}. Molar extinction coefficient (ε, m^2/mol): 2150 (300 nm), 550 (346 nm). Melting point: 233 °C.

Synthesis of 2b. 9-phenylcarbazole (0.24 g, 1 mmol) and OPhSOH (0.95 g, 2.1 mmol) were dissolved in anhydrous dichloromethane solution (100 mL). Then, the $BF_3\cdot Et_2O$ (0.42 g, 3 mmol) was added slowly into the reaction mixture. Large amount of water was added to quench reaction after 8 h, and extracted with dichloromethane. The combined organic abstract was dried over anhydrous MgSO4 and filtered. The solution was evaporated under vacuum condition and the crude product was purified by silica gel column chromatography to afford white solid 2b (0.72 g) with 64.9% yield. 1H NMR (400 MHz, $CDCl_3$) δ 8.19 (dd, J = 7.6, 1.2 Hz, 4H), 7.54–7.50 (m, 8H), 7.44 (m, 5H), 7.24 (d, J = 9.0 Hz, 2H), 7.16 (d, J = 2.0 Hz, 2H), 7.07 (d, J = 8.0 Hz, 1H), 6.79 (dd, J = 8.8, 2.0 Hz, 2H), 6.76–6.72 (m, 4H), 6.70–6.66 (m, 4H), 3.93 (t, J = 6.8 Hz, 4H), 1.83–1.73 (m, 4H), 1.50–1.40 (m, 4H), 1.34–1.24 (m, 16H), 0.87 (t, J = 6.8 Hz, 6H). 13C NMR (100 MHz, $CDCl_3$) δ 158.13, 146.10, 140.08, 137.33, 137.24, 136.60, 136.49, 132.03, 131.63, 131.45, 129.82, 128.29, 127.82, 127.55, 126.72, 124.01, 122.84, 122.06, 113.76, 109.46, 68.00, 58.50, 31.81, 29.38, 29.35, 29.24, 26.13, 22.65, 14.10. MALDI-TOF MS: calculated for $C_{72}H_{69}NO_6S_2$ 1108.45; found: 1107.25 (M+). Elemental analysis calculated for $C_{72}H_{69}NO_6S_2$: C, 78.02%; H, 6.27%; N, 1.26%; O, 8.66%; S, 5.79%. Found: C, 78.31%; H, 6.15%; N, 1.50%. IR (KBr): υ = 3063 (aryl CH), 2926 (CH_2, CH_3), 2853 (CH_2, CH_3), 1606 (Aryl C=C), 1506 (Aryl C=C), 1467 (Aryl C=C), 1440 (Aryl C=C), 1307 ($-SO_2-$), 1249 (Ar-O-R), 1169 ($-SO_2-$), 1056, 827, 759, 700, 594, 582 cm^{-1}. Molar extinction coefficient (ε, m^2/mol): 3288 (305 nm), 700 (353 nm). Melting point: 298 °C.

Synthesis of 1a. The synthetic procedure is similar to 1b, and afford light yellow solid product (0.32 g) with 79.5% yield. 1H NMR (400 MHz, $CDCl_3$) δ 8.23 (dd, J = 7.6, 1.2 Hz, 2H), 7.87 (d, J = 8.0 Hz, 1H), 7.59–7.54 (m, 7H), 7.48 (t, J = 8.0, 1.2 Hz, 3H), 7.39 (d, J = 7.6 Hz, 2H), 7.30–7.28 (m, 4H), 7.21 (td, J = 7.2, 1.6 Hz, 2H), 7.12 (d, J = 8.0 Hz, 2H), 6.88 (dd, J = 7.2, 1.6 Hz, 2H), 6.84 (dd, J = 8.8, 2.0 Hz, 1H). MALDI-TOF MS: calculated for $C_{37}H_{25}NO_2S$ 547.66; found: 547.05 (M+). Elemental analysis calculated for $C_{37}H_{25}NO_2S$: C, 81.14%; H, 4.60%; N, 2.56%; O, 5.84%; S, 5.85%. Found: C, 81.04%; H, 4.81%; N, 2.33%. IR (KBr): υ = 3057 (aryl CH), 1597 (Aryl C=C), 1502 (Aryl C=C), 1471 (Aryl C=C), 1448 (Aryl C=C), 1358, 1328, 1288 ($-SO_2-$), 1230 (Ar-N-Ar), 1165 ($-SO_2-$), 1057, 813, 761, 748, 732, 702, 650, 594.571 cm^{-1}. Molar extinction coefficient (ε, m^2/mol): 2125 (299 nm), 513 (346 nm). Melting point: over 185 °C.

Synthesis of 2a. The synthetic procedure is similar to 2b, and afford white solid product (0.88 g) with 74.3% yield. 1H NMR (400 MHz, $CDCl_3$) δ 8.21 (dd, J = 7.6, 1.2 Hz, 4H), 7.55–7.52 (m, 8H), 7.45 (td, J = 8.0, 1.2 Hz, 5H), 7.29–7.27 (m, 4H), 7.25–7.22 (m, 4H), 7.12 (d, J = 1.6, Hz, 2H), 7.06 (d, J = 7.6 Hz, 4H), 6.83–6.81 (m, 6H). 13C NMR (100 MHz, $CDCl_3$) δ145.82, 145.82, 144.63, 144.63, 140.11, 137.37, 137.28, 136.41, 132.13, 131.65, 130.25, 129.88, 128.59, 128.04, 127.94, 127.66, 127.22, 126.75, 124.07, 122.73, 122.24, 109.66, 59.12. MALDI-TOF MS: calculated for $C_{56}H_{37}NO_4S_2$ 852.03; found: 851.06 (M+). Elemental analysis calculated for $C_{56}H_{37}NO_4S_2$: C, 78.94%; H, 4.38%; N, 1.64%; O, 7.51%; S, 7.53%. Found: C, 79.12%; H, 4.45%; N, 2.01%. IR (KBr): υ = 3061 (aryl CH), 1597 (Aryl C=C), 1500 (Aryl C=C), 1487 (Aryl C=C), 1440 (Aryl C=C), 1365, 1307 ($-SO_2-$), 1237 (Ar-N-Ar), 1167 ($-SO_2-$), 1147, 1128, 1056, 810, 758, 738, 698, 594, 571 cm^{-1}. Molar extinction coefficient (ε, m^2/mol): 2750 (305 nm), 650 (350). Melting point: 320 °C.

Synthesis of 1c. The synthetic procedure is similar to 2a, and afford light yellow solid product (0.92 g) with 93% yield. 1H NMR (400 MHz, $CDCl_3$) δ 8.37 (d, J = 1.2 Hz, 1H), 8.25 (dd, J = 7.6, 1.2 Hz, 2H), 8.21 (d, J = 8.0 Hz, 1H), 8.15 (d, J = 1.2 Hz, 1H), 7.75 (dd, J = 8.4, 1.2 Hz, 1H), 7.69–7.60 (m, 10H), 7.57 (d, J = 8.0 Hz, 2H), 7.54–7.43 (m, 9H), 7.33 (d, J = 8.4 Hz, 1H), 7.31–7.28 (m, 4H), 7.17 (d, J = 7.6 Hz, 1H), 6.92 (d, J = 7.6 Hz, 1H), 6.91 (d, J = 7.6 Hz, 1H), 6.86 (dd, J = 8.8, 2.0 Hz, 1H). 13C NMR (100 MHz, $CDCl_3$) δ 146.17, 144.44, 141.37, 140.47, 140.28, 140.06, 137.75, 137.56, 137.46, 136.64, 134.72, 134.22, 132.17, 131.76, 130.21, 129.93, 128.76, 128.18, 127.97, 127.59, 127.49, 127.34, 127.08, 126.92, 126.24, 126.10, 125.86, 124.10, 123.92, 123.76, 123.50, 123.11, 122.59, 120.43, 120.00, 119.00, 118.98, 110.22, 109.97, 109.92, 109.47, 59.31. MALDI-TOF MS: calculated for $C_{55}H_{36}N_2O_2S$ 788.95; found: 788.04 (M+). Elemental analysis calculated for $C_{55}H_{36}N_2O_2S$: C, 83.73%; H, 4.60%; N, 3.55%; O, 4.06%; S, 4.06%. Found: C, 83.53%; H, 4.65%; N, 3.29%. IR (KBr): υ = 3061 (aryl CH), 1597 (Aryl C=C), 1500 (Aryl C=C), 1471 (Aryl C=C), 1444 (Aryl C=C), 1361, 1294 ($-SO_2-$), 1229 (Ar-N-Ar), 1168 ($-SO_2-$), 1147, 1130, 1059, 804, 790, 760, 700, 570 cm^{-1}. Molar extinction coefficient (ε, m^2/mol): 4782 (304 nm), 507 (356 nm). Melting point: 355 °C.

Synthesis of 2c. The synthetic procedure is similar to 2b, and afford white solid product (0.95 g) with 77% yield. 1H NMR (400 MHz, $CDCl_3$) δ 8.25 (dd, J = 7.6, 1.2 Hz, 4H), 8.07 (d, J = 1.2 Hz, 2H), 7.65 (dd, J = 8.4, 1.2 Hz, 2H), 7.63–7.60 (m, 10H), 7.56 (t, J = 7.6 Hz, 4H), 7.51–7.45 (m, 8H), 7.32 (d, J = 8.8 Hz, 2H), 7.30–7.27 (m, 6H), 7.15 (d, J = 8.0 Hz, 4H), 6.92–6.89 (m, 4H), 6.86 (dd, J = 8.4, 2.0 Hz, 2H). 13C NMR (101 MHz, $CDCl_3$) δ 146.15, 144.44, 140.47, 140.26, 137.48, 137.44, 136.59, 134.53, 132.16, 131.75, 130.21, 129.94, 128.76, 128.16, 127.95, 127.62, 127.32, 126.90, 126.24, 124.10, 123.67, 123.01, 122.57, 119.05, 110.15, 109.47, 59.29. MALDI-TOF MS: calculated for $C_{74}H_{48}N_2O_4S_2$ 1093.31; found: 1092.05 (M+). Elemental analysis calculated for $C_{74}H_{48}N_2O_4S_2$: C, 81.29%; H, 4.43%; N, 2.56%; O, 5.85%; S, 5.87%. Found: C, 81.13%; H, 4.29%; N, 2.41%. IR (KBr): υ = 3061 (aryl CH), 1595 (Aryl C=C), 1500 (Aryl C=C), 1470 (Aryl C=C), 1440(Aryl C=C), 1359, 1307 ($-SO_2-$), 1232 (Ar-N-Ar), 1170 ($-SO_2-$), 1147, 1130, 1057, 808, 758, 698, 594, 572 cm^{-1}. Molar extinction coefficient (ε, m^2/mol): 4938 (310 nm), 513 (359 nm). Melting point: 340 °C.

Synthesis of 1d. The synthetic procedure is similar to 2a, and afford light yellow solid product (0.78 g) with 85% yield. 1H NMR (400 MHz, $CDCl_3$) δ 8.37 (s, 1H), 8.27–8.16 (m, 4H), 7.74 (dd, J = 8.4, 1.6 Hz, 1H), 7.69 (m, 2H), 7.65–7.58 (m, 8H), 7.55 (td, J = 7.6, 1.2 Hz, 2H), 7.52–7.46 (m, 8H), 7.35–7.28 (m, 2H), 7.17 (d, J = 7.6 Hz, 2H), 6.86 (dd, J = 8.7, 1.6 Hz, 1H), 6.79 (s, 4H), 3.92 (t, J = 6.4 Hz, 2H), 1.81–1.71 (m, 2H), 1.47–1.37 (m, 2H), 1.32–1.23 (m, 8H), 0.87 (t, J = 6.8 Hz, 3H). 13C NMR (100 MHz, $CDCl_3$) δ 158.09, 146.43, 141.36, 140.45, 140.24, 140.05, 137.76, 137.58, 137.32, 136.97, 136.18, 134.69, 134.23, 132.04, 131.74, 131.29, 129.91, 128.70, 127.85, 127.55, 127.47, 127.08, 126.92, 126.19, 126.07, 125.90, 124.04, 123.91, 123.79, 123.50, 123.07, 122.48, 120.45, 119.97, 119.03, 118.97, 113.94, 110.17, 109.96, 109.88, 109.40, 67.97, 58.69, 31.79, 29.35, 29.29, 29.21, 26.07, 22.64, 14.09. MALDI-TOF MS: calculated for $C_{63}H_{52}N_2O_3S$ 917.16; found: 916.31 (M+). Elemental analysis calculated for $C_{63}H_{52}N_2O_3S$: C, 82.50%; H, 5.71%; N, 3.05%; O, 5.23%; S, 3.50%. Found: C, 82.31; H, 5.70; N, 3.28%. IR (KBr): υ = 3061 (aryl CH), 2924 (CH_3, CH_2), 2854 (CH_3, CH_2), 1597 (Aryl C=C), 1500 (Aryl C=C), 1470 (Aryl C=C), 1446 (Aryl C=C), 1361, 1305 ($-SO_2-$), 1249 (Ar-O-R), 1230 (Ar-N-Ar), 1168 ($-SO_2-$), 1057, 804, 760, 698, 582 cm^{-1}. Molar extinction coefficient (ε, m^2/mol): 6663 (305 nm), 700 (355 nm). Melting point: over 320 °C.

Synthesis of 2d. The synthetic procedure is similar to 2b, and afford white solid product (0.88 g) with 70.4% yield. 1H NMR (400 MHz, $CDCl_3$) δ 8.23 (dd, J = 7.6, 1.2 Hz, 4H), 8.07 (d, J = 1.2 Hz, 2H), 7.67–7.63 (m, 4H), 7.61–7.57 (m, 8H), 7.54 (td, J = 7.6, 1.2 Hz, 4H), 7.50–7.44 (m, 8H), 7.30 (d, J = 8.8 Hz, 2H), 7.14 (d, J = 7.6 Hz, 4H), 6.85 (dd, J = 8.8, 2.0 Hz, 2H), 6.80–6.74 (m, 8H), 3.92 (t, J = 6.8 Hz, 4H), 1.79–1.70 (m, 4H), 1.41 (m, 4H), 1.33–1.22 (m, 16H), 0.87 (t, J = 6.8 Hz, 6H). 13C NMR (100 MHz, $CDCl_3$) δ 158.07, 146.42, 140.44, 140.22, 137.53, 137.31, 136.92, 136.20, 134.56, 132.04, 131.73, 131.29, 129.90, 128.70, 127.83, 127.57, 126.90, 126.28, 124.03, 123.69, 123.00, 122.45, 119.13, 113.94, 110.10, 109.38, 67.95, 58.68, 31.80, 29.36, 29.31, 29.22, 26.07, 22.64, 14.09. MALDI-TOF MS: calculated for $C_{90}H_{80}N_2O_6S_2$ 1349.74; found: 1349.31 (M+). Elemental analysis calculated for $C_{90}H_{80}N_2O_6S_2$: C, 80.09%; H, 5.97%; N, 2.08%; O, 7.11%; S, 4.75%. Found: C, 79.82%; H, 6.17%; N, 2.15%. IR (KBr): υ = 3063 (aryl CH), 2926 (CH_3, CH_2), 2853 (CH_3, CH_2), 1597 (Aryl C=C), 1502 (Aryl C=C), 1470 (Aryl C=C), 1439 (Aryl C=C), 1361, 1307 ($-SO_2-$), 1248 (Ar-O-R), 1134 (Ar-N-Ar), 1168 ($-SO_2-$), 1147, 1128, 1057, 873, 806, 758, 698, 572 cm^{-1}. Molar extinction coefficient (ε, m^2/mol): 7175 (310 nm), 700 (359 nm). Melting point: 329 °C.

Synthesis of 1e. The synthetic procedure is similar to 2a, and afford white solid product (0.56 g) with 87% yield. 1H NMR

(400 MHz, $CDCl_3$) δ 8.23 (dd, $J = 7.6$, 1.2 Hz, 2H), 8.15 (d, $J = 7.6$ Hz, 2H), 7.88 (d, $J = 7.6$ Hz, 1H), 7.85–7.81 (m, 2H), 7.72–7.67 (m, 2H), 7.56–7.53 (m, 4H), 7.50 (d, $J = 8.0$ Hz, 2H), 7.47 (td, $J = 7.6$, 1.6 Hz, 2H), 7.45–7.41 (m, 4H), 7.32–7.22 (m, 6H), 7.11 (d, $J = 8.0$ Hz, 2H), 6.89–6.86 (m, 3H). 13C NMR (101 MHz, $CDCl_3$) δ 146.05, 144.44, 141.03, 140.69, 139.49, 139.43, 139.20, 137.49, 137.02, 132.14, 131.79, 131.31, 130.23, 128.89, 128.22, 128.02, 127.38, 126.51, 126.22, 126.09, 125.74, 125.23, 124.14, 123.62, 123.47, 123.15, 122.61, 120.56, 120.52, 120.39, 109.93, 109.67, 109.40, 59.29. MALDI-TOF MS: calculated for $C_{49}H_{32}N_2O_2S$ 712.86; found: 712.10 (M+). Elemental analysis calculated for $C_{49}H_{32}N_2O_2S$: C, 82.56%; H, 4.52%; N, 3.93%; O, 4.49%; S, 4.50%. Found: C, 82.23%; H, 4.34%; N, 3.79%. IR (KBr): υ = 3061 (aryl CH), 1560 (Aryl C=C), 1497 (Aryl C=C), 1448 (Aryl C=C), 1334, 1303 (–SO_2–), 1230 (Ar-N-Ar), 1166 (–SO_2–), 1147, 1057, 790, 750, 700, 650, 594, 570 cm^{-1}. Molar extinction coefficient (ε, m^2/mol): 4538 (293 nm), 1012 (341 nm). Melting point: 307 °C.

Synthesis of 2e, 2e′ and 3e. The synthetic procedure is similar to 2b, and afford white solid product 2e and 2e′ (0.74 g) and white solid 3e (0.17 g). The isomers of 2e and 2e′ cannot be purified via column chromatography, and the ratio of 2e to 2e′ is about 5:1 evaluating from 1H NMR spectra. 1H NMR spectra data of 3e: 1H NMR (400 MHz, $CDCl_3$) δ 8.23–7.19 (m, 6H), 7.86 (d, $J = 7.6$ Hz, 1H), 7.78 (s, 1H), 7.76 (t, $J = 8.0$ Hz, 1H), 7.66–7.63 (m, 2H), 7.59–7.51 (m, 7H), 7.48–7.34 (m, 11H), 7.31–7.20 (m, 10H), 7.12–7.09 (m, 4H), 7.03 (d, $J = 8.0$ Hz, 4H), 6.87 (dd, $J = 7.6$, 1.2 Hz, 2H), 6.83 (dd, $J = 8.8$, 1.6 Hz, 3H), 6.79 (d, $J = 7.6$ Hz, 4H). MALDI-TOF MS: calculated for $C_{87}H_{56}N_2O_6S_3$ 1321.58; found: 1321.15 (M+). Elemental analysis calculated for $C_{87}H_{56}N_2O_6S_3$: C, 79.07%; H, 4.27%; N, 2.12%; O, 7.26; S, 7.28%. Found: C, 79.25%; H, 4.11%; N, 2.42%. IR (KBr): υ = 3061 (aryl CH), 1599 (Aryl C=C), 1492 (Aryl C=C), 1456 (Aryl C=C), 1440 (Aryl C=C), 1307 (–SO_2–), 1236 (Ar-N-Ar), 1166 (–SO_2–), 1147, 1126, 1057, 806, 756, 732, 700, 594, 572 cm^{-1}. Molar extinction coefficient (ε, m^2/mol): 4062 (299 nm), 825 (345 nm).

2.3. Device fabrication and testing

Solution-processed OLEDs were fabricated with the configuration of indium tin oxide (ITO)/poly(ethylenedioxythiophene)-poly(styrenesulfonic acid) (PEDOT:PSS, 20 nm)/emissive layer (~40 nm)/1,3,5-tri[(3-pyridyl)-phen-3-yl]benzene (TmPyPB, 60 nm)/LiF (0.8 nm)/Al (100 nm). PEDOT:PSS layer with a thickness of 20 nm was spin-coated directly onto pre-cleaned ITO glass at a spin speed of 3000 rpm for 60 s, and dried at 120 °C for 20 min under vacuum condition. The Firpic and dye were dissolved in chlorobenzene with a concentration of 2 and 15 mg/mL, respectively, and then different weight ratio of Firpic/dye were prepared. Then the emissive layer was spin-coated onto top of PEDOT:PSS layer from Firpic/dye chlorobenzene solution and annealed at 100 °C for 20 min to remove residual solvents. TmPyPB, LiF and Al cathode were successively vacuum-deposited under the pressure lower than 5×10^{-4} pa in order of device configuration, respectively. The thickness of organic films was measured using a spectroscopic ellipsometry (α-SE, J.A.Wollam Co. Inc.). The current density-voltage-luminance characteristics were measured by a Keithley 2602 source meter with a calibrated silicon photodiode. The electroluminescence spectra of devices were analyzed with a spectrometer PR655. All device characterizations were carried out under ambient laboratory air at room temperature. The emission area of the devices is 12 mm^2.

3. Results and discussion

3.1. Synthesis and thermal behaviours

The synthetic routes of the key sulfone-contained tertiary alcohols, 9-hydroxy-9-phenylthioxanthene-10,10-dioxide (PhSOH) and 9-hydroxy-9-(4-(octyloxy)phenyl)thioxanthene-10,10-dioxide (OPhSOH), are shown in Scheme 1. Due to directed *ortho*-metalation of sulfone group, dilithation of diphenyl sulfone was performed well under treating diphenyl sulfone with 2.1 equivalent *n*-butyllithium [35]. Then, using methyl benzoate or 4-octoxylbenzoate to trap the dilithation, and affording PhSOH and OPhSOH with high yield of 88% and 72.1%, respectively. In order to study the reactivity of PhSOH and OPhSOH, we chose 9-phenylcarbazole (PhCz) as a D synthon and used our previous reaction condition of FC arylmethylation [19,36]. Fortunately, the reaction ran very well under mild $BF_3 \cdot Et_2O$ catalyst, which is quite different from strong protonic acid-catalyzed 9-aryl-4,5-diazofluoren-9-ol and 9-pyridine-2-ylfluoren-9-ol [12,24]. Due to electron-accepting effect, carbazole group is deactivated by sulfone group, mono- or di-substitution of phenylcarbazole (PhCz) can be easily controlled by adjusting the loading ratio of D and A, and afford 1a, 2a, 1b, and 2b with high yield of 79.5%, 74.3%, 91% and 64.9%, respectively. Since bicarbazole derivatives, 9,9′-diphenyl-3,3′-bicarbazole (DPhBCz) and 1,3-biscarbazol-9-ylbenzene (mCP), are typical and frequently used unipolar host materials, they can be functionalized easily by PhSOH and OPhSOH, and afford corresponding mono-, di- or tri-substituted derivatives. In addition, di-substituted mCP has two isomers, 2e and 2e′, and the ratio 2e to 2e′ is about 5:1 (evaluating from 1H NMR, Fig. S31). The chemical structures of the compounds were confirmed by FT-IR spectra, 1H and 13C NMR spectra, and MALDI-TOF mass spectra. Sulfone-substituted derivatives show high thermal decomposition temperature (T_d), the values are all higher than 390 °C (Table 1, Figs. S35–S39). In addition, the glass transition temperatures (T_g) of 1c, 2c, 2d and 1e, are 202, 250, 172 and 178 °C, respectively, and the other derivatives do not show obvious T_g, indicating sulfone-substituted derivatives have outstanding thermal and morphologic stability.

3.2. Crystal structures

Single crystals of PhSOH, OPhSOH, and 1b–1e were obtained at ambient temperature by slowly evaporating chloroform/n-hexane solution. 1e belongs to monoclinic system with P21/c group, and the others belong to triclinic system with P-1 group (Fig. 1 and Table S1 and S2). Since sulfone group is a good hydrogen acceptor, strong hydrogen bonds form in PhSOH and OPhSOH with the distance of O–H⋯O=S of 1.994 and 2.053 Å, respectively (Figs. S40 and S41). Thioxanthene-10,10-dioxide moiety adopts a butterfly-shaped structure and bend along the S-C9 axis. The dihedral angles between the two benzene rings of Thioxanthene-10,10-dioxide moiety are 21.83°, 29.99°, 36.91°, 24.18°, 39.46°, and 30.33° in PhSOH, OPhSOH, 1b, 1c, 1d and 1e, respectively. In addition, 1e shows two crystallographically independent conformations and adopts alternative arrangement and layered packing pattern in crystal (Figs. S42 and S43). As seen in 1b–1e, due to sterically hindered sulfone group, and sp^3-hybridized C connection of D and A moieties, the sulfone functionalized derivatives adopt twisted and non-planar 3D structures, which can effectively suppress intermolecular interactions and form stable amorphous films.

3.3. Photophysical properties

In order to investigate the effect of the functionalization of sulfone groups on photophysical properties, absorption, emission and low temperature phosphorescence were measured, and their spectra are shown in Fig. 2 and key data are listed in Table 1. Comparison with parent compounds, the absorption and emission of sulfone functionalization show bathochromic shift within 10 nm,

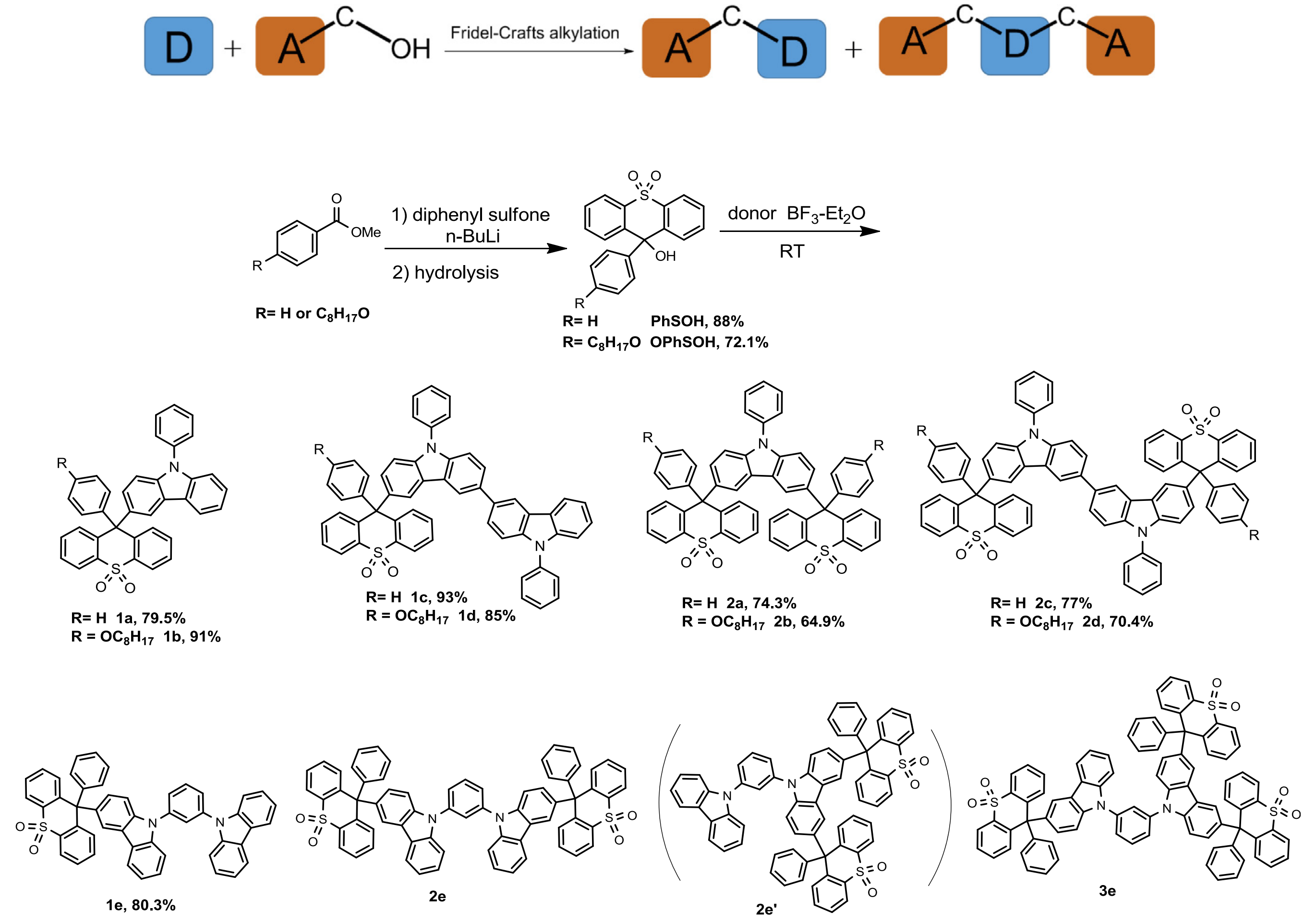

Scheme 1. Synthesis of sulfone-contained tertiary alcohols, PhSOH and OPhSOH, and sulfone-substituted carbazole, bicarbazole and mCP derivatives. Donor includes 9-phenylcarbazole, 9,9′-diphenyl-3,3′-bicarbazole and 1,3-biscarbazol-9-ylbenzene. It exists two isomers in di-sulfone-substitution of mCP (2e and 2e′), and the ratio 2e to 2e′ is about 5:1.

Table 1
Physical properties of PhCz, DPhBCz, and mCP, and their sulfone-substituted derivatives.

Entry	$T_g/T_m/T_d$[a] (°C)	λ_{abs}[b] (nm)	λ_{em}[b] (nm)	λ_{ph}[c] (nm)	HOMO[d] (eV)	LUMO[e] (eV)	E_g[f] (eV)	E_T[g] (eV)
PhCz	NM	293,327,340	350,364	411,440	−5.63	−2.07	3.56	3.02
1a	no/no/410	299,333,346	358,371	419,448	−5.68	−2.20	3.48	2.96
2a	no/no/402	305,336,350	363,375	420,448	−5.70	−2.28	3.42	2.95
1b	no/233/397	300,334,346	357,371	419,447	−5.70	−2.22	3.48	2.96
2b	no/298/393	305,336,353	365	420,448	−5.69	−2.26	3.43	2.95
DPhBCz	NM	304,353	407,429	449,479	−5.34	−1.94	3.40	2.76
1c	202/353/496	304,356	412,433	454,480	−5.35	−2.00	3.35	2.73
2c	250/no/433	310,359	413,438	456,484	−5.38	−2.06	3.32	2.72
1d	no/no/404	305,355	412,438	454,483	−5.37	−2.01	3.36	2.73
2d	172/329/425	310,359	414,437	456,483	−5.39	−2.05	3.34	2.72
mCP	NM	293,326,340	346,361	412,440	−5.72	−2.14	3.58	3.01
1e	178/307/504	293,327,341	354,369	418,446	−5.73	−2.22	3.51	2.97
2e(2e')	NM	298,331,344	356,370	418,447	−5.74	−2.24	3.50	2.97
3e	NM	299,333,345	360,373	419,448	−5.76	−2.29	3.47	2.96

[a] T_g: glass transition temperature; T_m: melting point temperature; T_d: decomposition temperature; NM: not measurement.

[b] Measured in dichloromethane solution.

[c] Measured in 2-MeTHF at 77 K.

[d] Determined from on-set oxidation potential in dichloromethane, and from equation, HOMO = $-(E_{on} - E_{\varphi})-4.80$ eV, where E_{φ} is on-set oxidation potential in dichloromethane, the value is 0.40 V vs Ag/AgCl.

[e] Evaluated from on-set reduction potential in tetrahydrofuran, and from equation, LUMO = $-(E_{on} - E_{\varphi})-4.80$ eV.

[f] Calculated from the equation E_g = LUMO-HOMO.

[g] Calculated from phosphorescence spectrum.

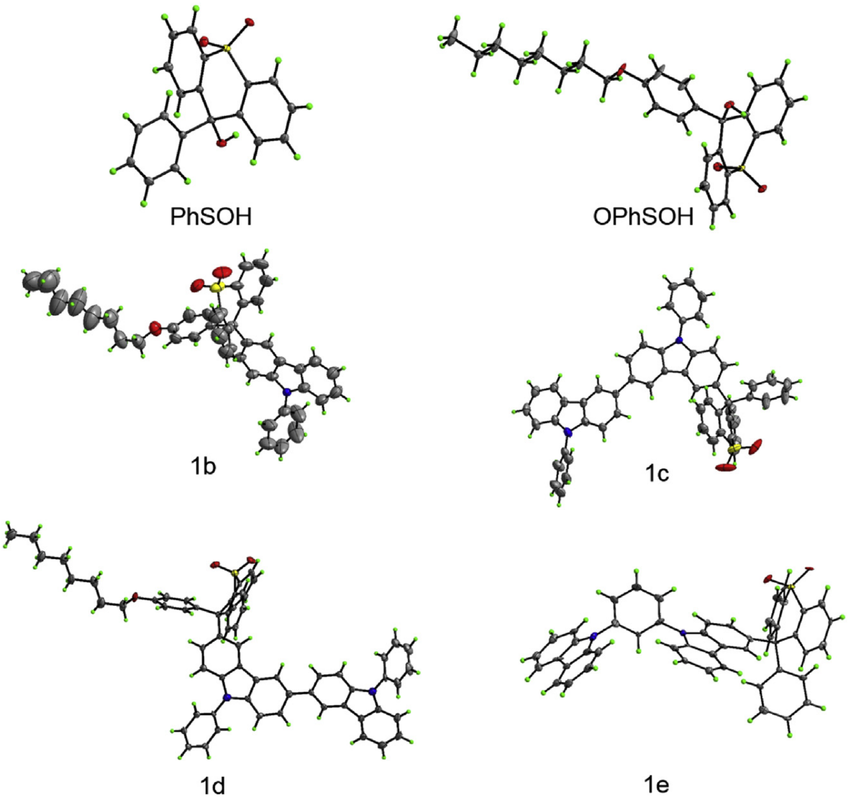

Fig. 1. ORTEP drawing (50% ellipsoid probability) of PhSOH, OPhSOH, and 1b–1e.

and the number of substitution also affects the red shift of absorption and emission spectra. While in phosphorescence, there is about 8 nm red-shift after sulfone functionalization, and spectra change a little with the change of the number of sulfone substitutions. All above results clearly indicate that the conjugation-interrupted link of D and A moieties has a weak electron coupling interaction, which makes sulfone-substituted derivatives keep high triplet energy (E_T). The E_T levels are about 2.96, 2.72 and 2.92 eV in the sulfone-functionalized PhCz, DPhBCz and mCP derivatives, respectively, and the drop of E_T is very small (less than 0.1 eV). The E_T is high enough for typical sky-blue phosphorescent emitter, bis [2-(4,6-difluorophenyl)pyridinato-C2,N](picolinato)iridium(III) (Firpic, E_T: 2.68 eV), so the sulfone-substituted derivatives can be used as host materials for Firpic-based sky-blue PhOLEDs.

3.4. Electrochemical properties

Electrochemical behaviors of sulfone-functionalized carbazole derivatives were probed by cyclic voltammetry. As shown in Fig. 3, S44 and Table 1, the sulfone-substituted derivatives and its parent compounds have similar on-set oxidation potentials, while the introduction of sulfone group can apparently lower the on-set reduction potentials, and the number of substitution has little influence on the on-set reduction potential. The electrochemical data indicate that the introduction electron-accepting sulfone groups have a little influence on the HOMO levels, while significantly lower the LUMO energy levels. Taking mCP and 1e for example, the LUMO level decreases from −1.84 eV of mCP to −2.12 eV of 1e. The fall of LUMO levels is beneficial to the injection of electron from electron-transporting layer. Theoretical calculation indicates that the introduction of sulfone group can effectively modulate the distribution of HOMO and LUMO energy levels (Fig. 4). The HOMO and LUMO levels separately locate on sulfone and carbazole moieties. Furthermore, sulfone functionalization significantly lower LUMO levels, while HOMO levels keep constant, which is consistent with the results evaluated from cyclic voltammetry. So using sulfone group to functionalize can effectively construct bipolar host materials for PhOLEDs or TADF OLEDs.

In addition, sulfone-substituted derivatives exhibit different electrochemical stability. PhCz exhibits irreversible oxidation process, and a new reduction peak around 0.90 V, indicating electrocoupling reaction takes place, and bicarbazole derivatives may form in this process (Fig. S45. Similarly, mono-substituted derivatives (1a and 1b) show the same behaviors as PhCz; while, di-substituted derivatives (2a and 2b) show reversible oxidation process, and exhibit well electrochemical stability under multiple CV scans (Figs. S46–S48), that means di-substitution of 3,6-position of carbazole can improve electrochemical stability of carbazole. DPhBCz and its sulfone-substitution derivatives display two well reversible oxidation peaks, implying that bicarbazole derivatives possess excellent electrochemical stability (Figs. S49–S53). mCP and its derivatives also show electrocoupling behaviors and irreversible oxidation process (Figs. S54–S57), indicating electrochemical stability of mCP derivatives is not very well.

3.5. Electroluminescent devices

To evaluate the applications of sulfone-functionalized carbazole derivatives as bipolar host materials, 1d and 1e were chosen as host materials to test feasibility, and fabricated solution-processed sky-blue phosphorescent devices using Firpic as a dopant. The device performances are shown in Fig. 5, S59 and the key parameters are summarized in Table 2. Fig. 5 shows current density-voltage-luminance curves, and current efficiency and power efficiency

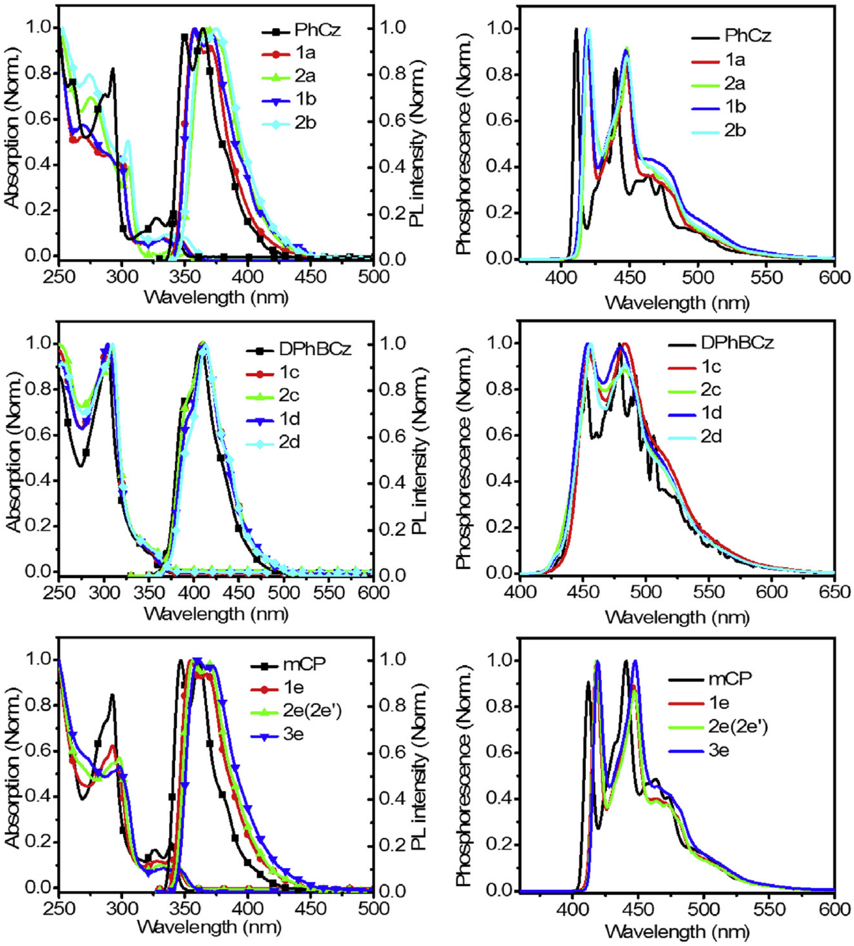

Fig. 2. Absorption, emission and phosphorescence spectra of sulfone-functionalized PhCz, DPhBCz and mCP derivatives. (Left column) Absorption and fluorescence were taken from dichloromethane solution at 10^{-5} mol/L at room temperature. (Right column) Phosphorescence was recorded in 2-MeTHF at 77 K.

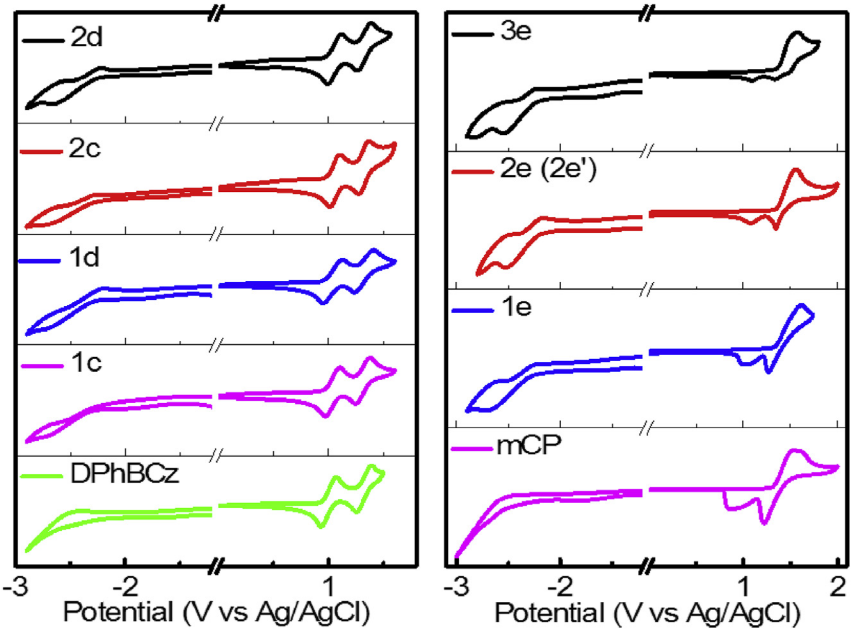

Fig. 3. Cyclic voltammograms of sulfone-functionalized DPhBCz and mCP derivatives in dichloromethane (oxidation) and tetrahydrofuran (reduction) solution with 0.1 M $TBAPF_6$ as the supporting electrolyte at the scanning of 0.1 V/s at room temperature.

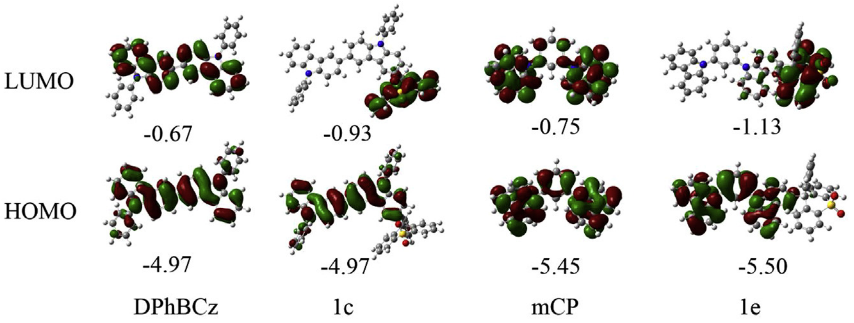

Fig. 4. The distribution of HOMO and LUMO energy levels, and its corresponding values of DPhBCz, 1c, mCP and 1e under B3LYP/6-31G(d) level.

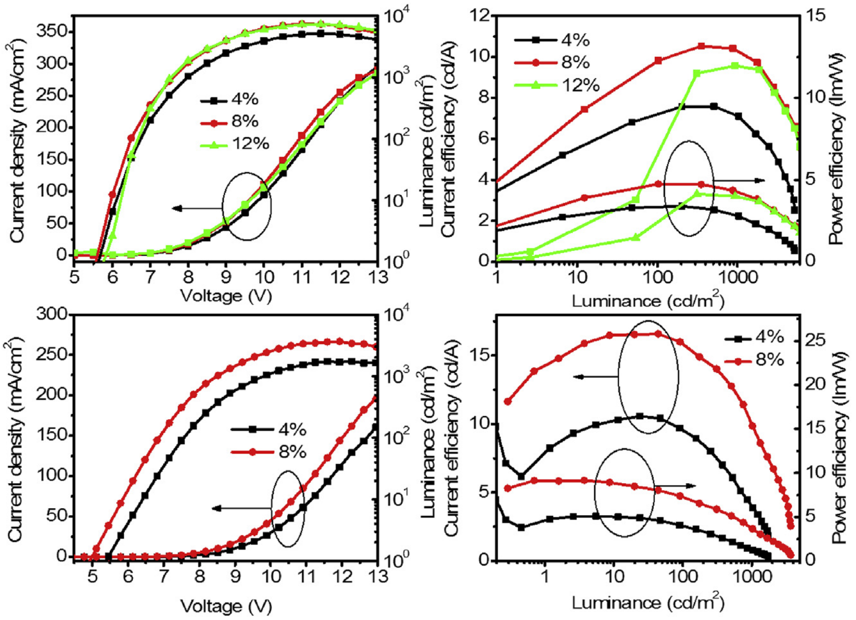

Fig. 5. Solution-processed Firpic-based electroluminescent performance using 1d and 1e as host materials. Current density-voltage-luminance curves, and current efficiency and power efficiency versus luminance curves based on 1d (top) and 1e (bottom).

Table 2
Summary of device performances of this work and literature.

Host	Von (V)	CE$_{max}$ (cd/A)	PE$_{max}$ (lm/W)	EQE$_{max}$ (%)	Ref.
mCP	8.2	11.5	3.6	2.4	This work
1d	5.6	10.5	4.7	3.8	This work
1e	5	16.5	9.2	7.2	This work
SPA-TXO2	2.9	30	19.8	11.4	25
p-DCz-SO2	2.6	31.5	32.3	15.6	26
m-DCz-SO2	2.8	30	33.7	13.4	26
EBCz-ThX	3.7	23	12.4	11.5	14
3	3.9	14.8	8.2	4.8	23

All the reported devices were fabricated via vacuum deposition using Firpic and sulfone derivatives as dopant and host materials, respectively.

versus luminance curves. The turn-on voltages (V$_{on}$) of 1d and 1e-based OLEDs are at the region of 5–6 V, and V$_{on}$ of 1e-based device is slightly lower than that of 1d. The device based on 1e exhibited a low current density, a maximum luminance of 3678 cd/m^2, and a maximum current efficiency (CE) of 16.5 cd/A at doping concentration of 8%. While the unmodified unipolar mCP-based device shows modest device performance with a maximum CE of 11.5 cd/A (Fig. S59). The device based on 1d shows high current density (more 2 times than 1e-based devices under same applied bias), and modest electroluminescent performance with a maximum CE of 10.5 cd/A. Hole-only and electron-only devices of 2d and 1e also were fabricated to compare hole and electron densities within emitting layers. As shown in Fig. S63, there are large difference in current densities in 2d-based hole-only and electron-only devices, while 1e shows small difference in hole and electron densities and balance carrier transporting property. That's the main reason why 1e-based device has better performance than 2d-based device. The above results indicates that sulfone-based bipolar host materials constructed via Friedel-Crafts reaction can effectively tune carrier-transporting characteristics of materials and improve device performance.

4. Conclusions

In summary, we have synthesized two sulfone-contained tertiary alcohols, and those A synthons can be used to construct bipolar host materials under mild one-step FC arylmethylation reaction. Using sulfone acceptors to functionalize can effectively modulate the distribution of HOMO and LUMO energy levels, and lower LUMO level, while keep high E$_T$. Efficient solution-processed sky-blue Firpic-based PhOLEDs were fabricated using sulfone-functionalized mCP as a bipolar host, and exhibited a maximum

CE of 16.5 cd/A. Those results demonstrate that FC arylmethylation is a powerful synthetic strategy to construct bipolar host materials.

Acknowledgements

The project was supported by the National Natural Science Funds for Excellent Young Scholar (21322402), National Natural Science Foundation of China (U1301243, 61136003), Doctoral Fund of Ministry of Education of China (20133223110007), Excellent Science and Technology Innovation Team of Jiangsu Higher Education Institutions (2013), Synergetic Innovation Center for Organic Electronics and Information Displays.

Appendix A. Supplementary data

Supplementary data related to this article can be found at http://dx.doi.org/10.1016/j.orgel.2016.08.018.

References

[1] S. Hirata, Y. Sakai, K. Masui, H. Tanaka, S.Y. Lee, H. Nomura, N. Nakamura, M. Yasumatsu, H. Nakanotani, Q. Zhang, Highly efficient blue electroluminescence based on thermally activated delayed fluorescence, Nat. Mater. 14 (2015) 330–336.

[2] C.W. Lee, J.Y. Lee, External quantum efficiency in blue phosphorescent organic light-emitting diodes using pyrido [2, 3-b] indole derivatives as host materials, Adv. Mater. 25 (2013) 5450–5454.

[3] H. Uoyama, K. Goushi, K. Shizu, H. Nomura, C. Adachi, Highly efficient organic light-emitting diodes from delayed fluorescence, Nature 492 (2012) 234–238.

[4] C. Han, L. Zhu, J. Li, F. Zhao, Z. Zhang, H. Xu, Z. Deng, D. Ma, P. Yan, Highly efficient multifluorenyl host materials with unsymmetrical molecular configurations and localized triplet states for green and red phosphorescent devices, Adv. Mater. 26 (2014) 7070–7077.

[5] S. Gong, Q. Fu, W. Zeng, C. Zhong, C. Yang, D. Ma, J. Qin, Solution-processed double-silicon-bridged oxadiazole/arylamine hosts for high-efficiency blue electrophosphorescence, Chem. Mater. 24 (2012) 3120–3127.

[6] S.O. Jeon, S.E. Jang, H.S. Son, J.Y. Lee, External quantum efficiency above 20% in deep blue phosphorescent organic light-emitting diodes, Adv. Mater. 23 (2011) 1436–1441.

[7] A. Chaskar, H.F. Chen, K.T. Wong, Bipolar host materials: a chemical approach for highly efficient electrophosphorescent devices, Adv. Mater. 23 (2011) 3876–3895.

[8] J.C. Xiao, B. Yang, J.I. Wong, Y. Liu, F.X. Wei, K.J. Tan, X. Teng, Y.C. Wu, L. Huang, C. Kloc, F. Boey, J. Ma, H. Zhang, H.Y. Yang, Q.C. Zhang, Synthesis, characterization, self-assembly and physical properties of 11-methylbenzo[*d*]pyreno[4, 5-*b*]furan, Org. Lett. 13 (2011) 3004–3007.

[9] H.H. Chou, C.H. Cheng, A highly efficient universal bipolar host for blue, green, and red phosphorescent OLEDs, Adv. Mater. 22 (2010) 2468–2471.

[10] Q.C. Zhang, Y. Divayana, J.C. Xiao, Z.J. Wang, E.R.T. Tiekink, H.M. Doung, H. Zhang, F. Boey, X.W. Sun, F. Wudl, Synthesis, characterization, and bipolar transporting behavior of a new twisted polycyclic aromatic hydrocarbon: 1′,4′-diphenyl-naphtho-(2′.3′:1.2)-pyrene-6′-nitro-7′-methyl carboxylate, Chem. Eur. J. 16 (2010) 7422–7426.

[11] S. Thiery, D. Tondelier, B. Geffroy, E. Jacques, M. Robin, R. Metivier, O. Jeannin, J. Rault-Berthelot, C. Poriel, Spirobifluorene-2,7-dicarbazole-4′-phosphine oxide as host for high-performance single-layer green phosphorescent OLED devices, Org. Lett. 17 (2015) 4682–4685.

[12] S. Gong, Y.-L. Chang, K. Wu, R. White, Z.-H. Lu, D. Song, C. Yang, High-power-efficiency blue electrophosphorescence enabled by the synergistic combination of phosphine-oxide-based host and electron-transporting materials, Chem. Mater. 26 (2014) 1463–1470.

[13] X. Yang, H. Huang, B. Pan, M.P. Aldred, S. Zhuang, L. Wang, J. Chen, D. Ma, Modified 4, 4′, 4″-Tri (N-carbazolyl) triphenylamine as a versatile bipolar host for highly efficient blue, orange, and white organic light-emitting diodes, J. Phys. Chem. C 116 (2012) 15041–15047.

[14] H. Liu, G. Cheng, D. Hu, F. Shen, Y. Lv, G. Sun, B. Yang, P. Lu, Y. Ma, A highly efficient, blue-phosphorescent device based on a wide-bandgap host/FIrpic: rational design of the carbazole and phosphine oxide moieties on tetraphenylsilane, Adv. Funct. Mater. 22 (2012) 2830–2836.

[15] C. Han, Z. Zhang, H. Xu, S. Yue, J. Li, P. Yan, Z. Deng, Y. Zhao, P. Yan, S. Liu, Short-axis substitution approach selectively optimizes electrical properties of dibenzothiophene-based phosphine oxide hosts, J. Am. Chem. Soc. 134 (2012) 19179–19188.

[16] C.-J. Zheng, J. Ye, M.-F. Lo, M.-K. Fung, X.-M. Ou, X.-H. Zhang, C.-S. Lee, New ambipolar hosts based on carbazole and 4, 5-diazafluorene units for highly efficient blue phosphorescent OLEDs with low efficiency roll-off, Chem. Mater. 24 (2012) 643–650.

[17] Y.P. Jeon, K.S. Kim, K.K. Lee, I.K. Moon, D.C. Choo, J.Y. Lee, T.W. Kim, Blue phosphorescent organic light-emitting devices based on carbazole/thioxanthene-S,S-dioxide with a high glass transition temperature, J. Mater. Chem. C 3 (2015) 6192–6199.

[18] C. Tang, R. Bi, Y. Tao, F. Wang, X. Cao, S. Wang, T. Jiang, C. Zhong, H. Zhang, W. Huang, A versatile efficient one-step approach for carbazole–pyridine hybrid molecules: highly efficient host materials for blue phosphorescent OLEDs, Chem. Commun. 51 (2015) 1650–1653.

[19] L.-H. Xie, X.-Y. Hou, Y.-R. Hua, C. Tang, F. Liu, Q.-L. Fan, W. Huang, Facile synthesis of complicated 9,9-Diarylfluorenes based on BF3·Et2O-mediated Friedel–Crafts reaction, Org. Lett. 8 (2006) 3701–3704.

[20] P.-I. Shih, C.-L. Chiang, A.K. Dixit, C.-K. Chen, M.-C. Yuan, R.-Y. Lee, C.-T. Chen, E.W.-G. Diau, C.-F. Shu, Novel carbazole/fluorene hybrids: host materials for blue phosphorescent OLEDs, Org. Lett. 8 (2006) 2799–2802.

[21] K.-T. Wong, Y.-M. Chen, Y.-T. Lin, H.-C. Su, C.-C. Wu, Nonconjugated hybrid of carbazole and Fluorene: a novel host material for highly efficient green and red phosphorescent OLEDs, Org. Lett. 7 (2005) 5361–5364.

[22] Z. Fan, H. Zhao, N. Li, Y. Quan, Q. Chen, S. Ye, S. Li, Y. Wang, Q. Fan, W. Huang, Tuning charge balance in solution-processable bipolar triphenylamine-diazafluorene host materials for phosphorescent devices, ACS Appl. Mater. Interfaces 7 (2015) 9445–9452.

[23] Y. Qian, Y. Ni, S. Yue, W. Li, Z. Zhang, L. Xie, M. Sun, Y. Zhao, W. Huang, Spiro fluorene-9,9′-xanthene -based universal hosts for understanding structure-property relationships in RGB and white PhOLEDs, RSC Adv. 5 (2015) 29828–29836.

[24] X.-H. Zhao, Z.-S. Zhang, Y. Qian, M.-D. Yi, L.-H. Xie, G.-H. Xie, H. Xu, C.-M. Han, Y. Zhao, A bulky pyridinylfluorene-functionalizing approach to synthesize diarylfluorene-based bipolar host materials for efficient red, green, blue and white electrophosphorescent devices, J. Mater. Chem. C 1 (2013) 3482–3490.

[25] Y. Qian, G. Xie, S. Chen, Y. Ni, X. Zhou, L. Xie, J. Liang, Y. Zhao, M. Yi, Y. Zhao, W. Wei, W. Huang, A new spiro[fluorene-9,9′-xanthene]-based host material possessing no conventional hole- and electron-transporting units for efficient and low voltage blue PHOLED via simple two-step synthesis, Org. Electron 13 (2012) 2741–2746.

[26] M. Romain, C. Quinton, D. Tondelier, B. Geffroy, O. Jeannin, J. Rault-Berthelot, C. Poriel, Thioxanthene and dioxothioxanthene dihydroindeno [2, 1-b] fluorenes: synthesis, properties and applications in green and sky blue phosphorescent OLEDs, J. Mater. Chem. C 4 (2016) 1692–1703.

[27] M. Romain, D. Tondelier, O. Jeannin, B. Geffroy, J. Rault-Berthelot, C. Poriel, Properties modulation of organic semi-conductors based on a donor-spiro-acceptor (D-spiro-A) molecular design: new host materials for efficient sky-blue PhOLEDs, J. Mater. Chem. C 3 (2015) 9701–9714.

[28] M. Romain, D. Tondelier, B. Geffroy, A. Shirinskaya, O. Jeannin, J. Rault-Berthelot, C. Poriel, Spiro-configured phenyl acridine thioxanthene dioxide as a host for efficient PhOLEDs, Chem. Commun. 51 (2015) 1313–1315.

[29] K. Liu, X.-L. Li, M. Liu, D. Chen, X. Cai, Y.-C. Wu, C.-C. Lo, A. Lien, Y. Cao, S.-J. Su, 9, 9-Diphenyl-thioxanthene derivatives as host materials for highly efficient blue phosphorescent organic light-emitting diodes, J. Mater. Chem. C 3 (2015) 9999–10006.

[30] Y. Li, Z. Wang, X. Li, G. Xie, D. Chen, Y.-F. Wang, C.-C. Lo, A. Lien, J. Peng, Y. Cao, Highly efficient spiro [fluorene-9, 9′-thioxanthene] core derived blue emitters and fluorescent/phosphorescent hybrid white organic light-emitting diodes, Chem. Mater. 27 (2015) 1100–1105.

[31] Z. Chen, X.-K. Liu, C.-J. Zheng, J. Ye, X.-Y. Li, F. Li, X.-M. Ou, X.-H. Zhang, A high-efficiency hybrid white organic light-emitting diode enabled by a new blue fluorophor, J. Mater. Chem. C 3 (2015) 4283–4289.

[32] S.O. Jeon, T. Earmme, S.A. Jenekhe, New sulfone-based electron-transport materials with high triplet energy for highly efficient blue phosphorescent organic light-emitting diodes, J. Mater. Chem. C 2 (2014) 10129–10137.

[33] C.-Y. Chan, Y.-C. Wong, M.-Y. Chan, S.-H. Cheung, S.-K. So, V.W.-W. Yam, Hole-transporting spirothioxanthene derivatives as donor materials for efficient small-molecule-based organic photovoltaic devices, Chem. Mater. 26 (2014) 6585–6594.

[34] J. Ye, Z. Chen, M.-K. Fung, C. Zheng, X. Ou, X. Zhang, Y. Yuan, C.-S. Lee, Carbazole/Sulfone hybrid D-π-A-structured bipolar fluorophores for high-efficiency blue-violet electroluminescence, Chem. Mater. 25 (2013) 2630–2637.

[35] A. Chopra, D.C. Dorton, C.A. Ogle, Directed ortho dilithiation of diaryl compounds: facile synthesis of tricyclic compounds based on heterocycles fused to two benzene rings, Main. Group Met. Chem. 20 (1997) 783–786.

[36] L.-H. Xie, X.-Y. Hou, C. Tang, Y.-R. Hua, R.-J. Wang, R.-F. Chen, Q.-L. Fan, L.-H. Wang, W. Wei, B. Peng, W. Huang, Novel H-Shaped persistent architecture based on a Dispiro building block system, Org. Lett. 8 (2006) 1363–1366.